

FINAL REPORT ON CONTRACT NAS8-36191

COSMIC RAY DETECTORS

by

John C. Gregory
Associate Professor
School of Science
Department of Chemistry
University of Alabama in Huntsville
Huntsville, AL 35899
(205)895-6028

(NASA-CR-179086) COSMIC RAY DETECTORS Final
Report (Alabama Univ.) 29 p Avail: NTIS
PC A03/MF A01 CSCI 14B

N87-22952

Unclas
G3/35 0064066

February 1987

FINANCIAL STATUS REPORT

CONTRACT NAS8-36191

As of 12/31/86

Total Cumulative Costs incurred as of \$53,739.47

Estimate of cost to complete 53,992.00

Estimated Percentage of Physical Completion 95.5%

Statement relating the Cumulative cost to the percentage of physical completion with explanation of any significant variance:

I. SUMMARY

The contract included work on the MSFC emulsion laboratory microscopes in which mechanical modifications previously made were verified, and a design study of a large area hybrid electronic/emulsion chamber balloon-flight detector system. This design built upon the experience obtained with the highly successful MSFC/UAH hybrid instrument flown by the JACEE consortium (designated JACEE-3). The design included overall system design and specification, design and fabrication of a prototype large light diffusion for Cerenkov charge detector or scintillator, design of a multi-wire proportional counter array and design of the gondola or flight support system.

II. MICROSCOPE DESIGN MODIFICATION

a) Design Modification to Microscopes in Emulsion Laboratory, MSFC

The vertical focusing of the microscope was modified to allow operator's manual control while achieving computer data-loading from the microscope. This was done by replacing the original screws and revolving knob with catapillar belt interfaced knob detouring down to the stem of the microscope, (Fig. a1). With this, the manual operation of focusing is achieved during coordinates data-loading for single-operator manipulation. Two microscopes were modified by the same design and fabrication.

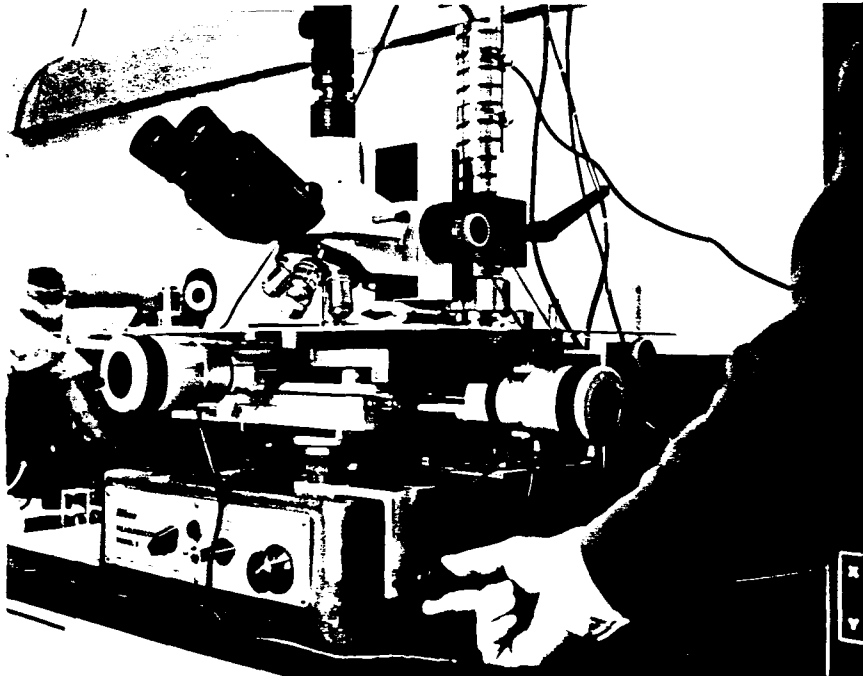


Figure q1

b) Verification of the Modified Microscopes

The modified microscope has been used for the event analyses. The digitized coordinates in (x,y,z) were used to predict the event location in subsequent plates. The Amiga computer provides instructions to bring a new plate to the exact predicted position of the event being followed. The interaction points have been traced with this system for the analysis of the latest emulsion chambers of the Japanese-American-Cooperative-Emulsion-Experiments (JACEE-6) which was flown in May, 1986. About 500 events were traced and the interactions were identified within two months of effort, which is about a factor of five quicker than using previous methods.

The storage of visual images of each frame was attempted so that more automated track analysis will become possible. However, the necessary frame-memory interface for the Amiga computer did not become available to the users by the time of the end of the present contract. This task will be carried over to future efforts.

III. DESIGN OF LARGE AREA HYBRID SYSTEM

Objectives

The primary objective of the experiment is to obtain 100 - 200 heavy nucleus interactions above 100 GeV/n for detailed analysis by emulsion techniques. The purpose of the electronic instrument, now well demonstrated by JACEE-3, is to permit the selection of the desired heavy nucleus events below the energy threshold of x-ray film spots in emulsion chambers without the work of tracing several thousand unwanted events. The electronic instrument must determine the charge and energy of each particle passing through the instrument and provide sufficiently accurate trajectory information so that events of particular interest can be located in the passive chambers. Though the burst counter provides a relatively poor energy measurement, its performance as a threshold energy detector has been demonstrated. Event statistics for the proposed instrument for a typical 30 hr flight are shown for two trigger levels in table 1. Numbers were calculated from

$$N = I >(E_o) \cdot SNT \cdot C_Z P_Z(E_o) \cdot P_{IZ}$$

where I is the primary integral spectrum, SNT is the exposure factor, C_Z the atmospheric transmission, P_Z the threshold function and P_{IZ} the interaction probability in the emulsion chamber.

An operational flight constraint of 5000 lbs including ballast (1800 lbs) was adopted, leaving the design goal of about 2000 lbs for emulsion chambers and 1200 lbs for the electronic detectors and mechanical support system (gondola). Since the pressurised-vessel gondola must be dispensed with because of its weight, all electronics and detectors must be designed for operation at ~5 Torr, at which pressure electrical and thermal problems must be addressed.

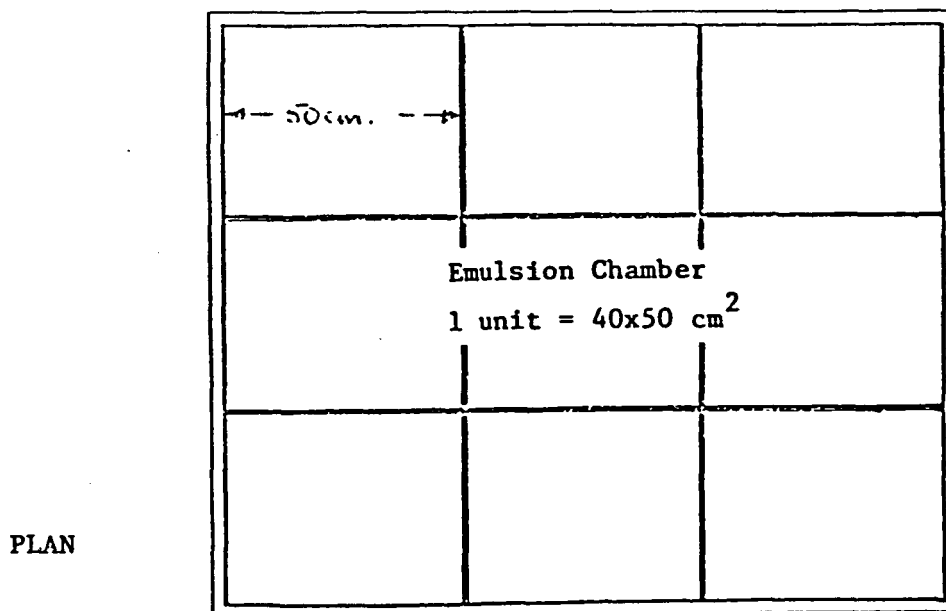
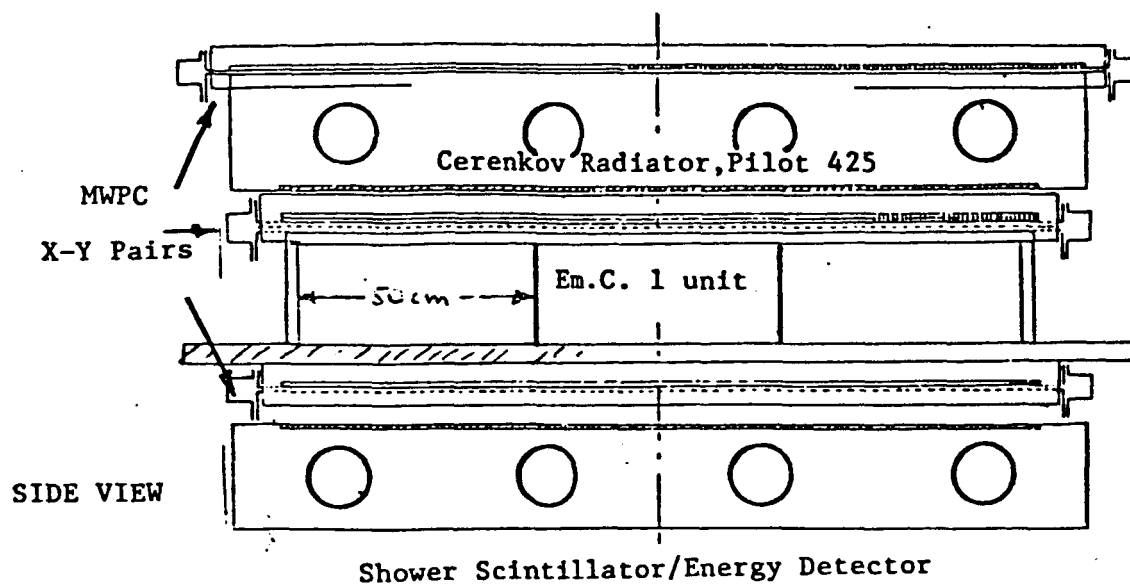


Figure 1. Large Area Hybrid Detector for Easy Selection of High Energy Heavy Cosmic Ray Interactions for Emulsion Chamber Analysis.

Table 1(a)

EXPECTED EVENT NUMBER IN EMULSION CHAMBER
 AT $\Sigma E_{\gamma}(\text{threshold}) = 1 \text{ TeV}$

	>200	>Eo (GeV/n) >500	>1000	>2000	Total No. of Triggered Events
Z \geq 17	40 (56)	10 (14)	3.1 (4.3)	0.9 (1.3)	62 (87)
Ne-S	61 (99)	31 (50)	9.8 (16)	3.3 (5.3)	61 (99)
C-O	74 (138)	60 (111)	25 (47)	8.6 (16)	74 (138)
H _e	72 (304)	72 (304)	63 (264)	34 (145)	72 (304)
P	230 (1100)	230 (1100)	230 (1100)	230 (1100)	230 (1100)
<u>TOTAL</u>					
Z \geq 6	175	101	38	13	197
all	477	403	331	277	500

xx: number interacting in chamber

(xx): number at top of chamber

*Exposure Factor: $SQT = 2.6 \times 10^5 \text{ m}^2 \text{ sr s}$

Table 1(b)

EXPECTED EVENT NUMBER IN EMULSION CHAMBER
 AT $\Sigma E_{\gamma}(\text{threshold}) = 3 \text{ TeV}$

Charge	>200	>Eo (GeV/n) >500	>1000	>2000	Total No. of Triggered Events
Z \geq 17	9.3 (13)	7.1 (10)	2.9 (4)	0.9 (1.3)	9.3 (13)
Ne-S	9.2 (15)	9.2 (15)	7.4 (12)	2.9 (4.8)	9.2 (15)
C-0	11 (21)	11 (21)	9.7 (18)	7.0 (13)	11 (21)
H _e	9.7 (41)	9.7 (41)	9.7 (41)	9.7 (41)	9.7 (41)
P	31 (150)	31 (150)	31 (150)	31 (150)	31 (150)
<u>TOTAL</u>					
Z \geq 6	30	27	20	11	30
all	70	68	61	52	70

xx: number interacting in chamber

(xx): number at top of chamber

The new instrument is shown in figure 1. It contains, apart from the emulsion chambers, the following elements which are discussed below in detail:

- A. Charge Detector
- B. Proportional Counter Hodoscope (PCH) for tracking
- C. Burst Counter for energy trigger
- D. Support Structure

A. Charge Detector

(i) Design Goals

Techniques for charge detection are now standard practice and no developments are needed. A new approach was required to the engineering of the box itself, since the area of the radiator is approximately 9 times that of JACEE-3.

The charge resolution design goal was $\sigma(z) \leq 1$. This was derived by equating with the practical resolution obtained with the other charge detector (CR-39) when the track-registration temperature is not known within a few degrees. The charge resolution is also controlled by the necessity to know the approximate charge for the burst counter interpretation.

(ii) Selection of Radiator

Both scintillators and Cerenkov radiators were considered as the light-emitter. Factors affecting the charge resolution obtainable with such materials includes: intrinsic photon production and fluctuations thereof, light collection efficiency, area non-uniformities, temperature dependency of photomultipliers (PMT's) and contamination of signal by back-flow of particles from an interaction in the emulsion chamber. The last effect was observed in JACEE-3 as an energy dependence of the charge

detector signal above 20 GeV/n for Fe particles. Because most of the back-scattered particles are known to be of low-energy, a Cerenkov radiator with threshold $\beta \approx 0.6$ was selected for this application since it is expected to be less sensitive to these particles than a scintillator.

(iii) Light Collection Efficiency and Charge Resolution

For a light diffusion box of total internal area A_t painted with white coating of reflectance r , and equipped with photomultipliers (PMT's) of total face-area A_p we may calculate the efficiency of collection of photons by the PMT's. Assumptions are that light emission (by Cerenkov or scintillation effect) is isotropic, that reflection from paint is diffuse and that no light is reflected from PMT faces.

Then, if $S = A_p/A_t$, the efficiency ϵ of collection is given by

$$\epsilon = s/(1-r(1-s))$$

The function ϵ is plotted versus r and s in figures 12 and 13 for practical values of r and s . The calculated values agree well with actual tests and calibrations made in the laboratory.

From figures 12 and 13 it may be seen that at reflectances $< .95$ small changes in reflectance are unimportant, while above $r = 0.97$ the efficiency improves markedly with small changes in r . As a practical matter even the best BaSO_4 paint if not properly applied may have a reflectance of .95, while if proper procedures are used 0.98 is attainable. The practical range of s is limited by cost and weight. For a detector of size 1 to 2 m on a side, s would be in the range of 0 to a few percent. For $s = 2.5\%$ we see that the collection efficiency ranges from 40 to 55% for paint

reflectances in the range 0.96 to 0.98. It should be noted that the presence of a solid radiator in the diffusion box may reduce the effective value of r below that of the reflectance coating. Measurements on a test diffusion box with $s = 0.7\%$ and measured efficiency ϵ of $\sim 10\%$ indicate (from figure 11) that the effective reflectance in this case was 0.94.

From results of a previous flight Cerenkov counter (CP-76) we obtain the comparison:

Counter	Radiator	$r(\text{eff.})$	$s\%$	ϵ	$n(\text{pe})$	σ_{pe} (charge units)
CP-76	$\frac{1}{2}$ " Pilot 425	0.94	3.7	0.38	21	0.11
design	$\frac{1}{4}$ " Pilot 425	0.94	2.6	0.29	7.3	0.19

Other sources of random signal variation exist however, affecting the resolution:

$$\sigma^2 = \sigma_{\text{pe}}^2 + \sigma_{\lambda}^2 + \sigma_{\text{sn}}^2 + \dots$$

where σ_{λ} is the path-length uncertainty and σ_{sn} that due to system noise. An estimate of variances other than photoelectron statistics based on actual flight experience yields an effective charge resolution for the new detector design of $\sigma(z) \sim 0.3$ charge units. This resolution is adequate for the purpose.

Mechanical Design of Light-Diffusion Boxes for Charge and Burst Detectors

The boxes must accommodate plastic radiators 150 cm square lying on the bottom (or fastened to the top) of the box and viewed by 12 PMT's

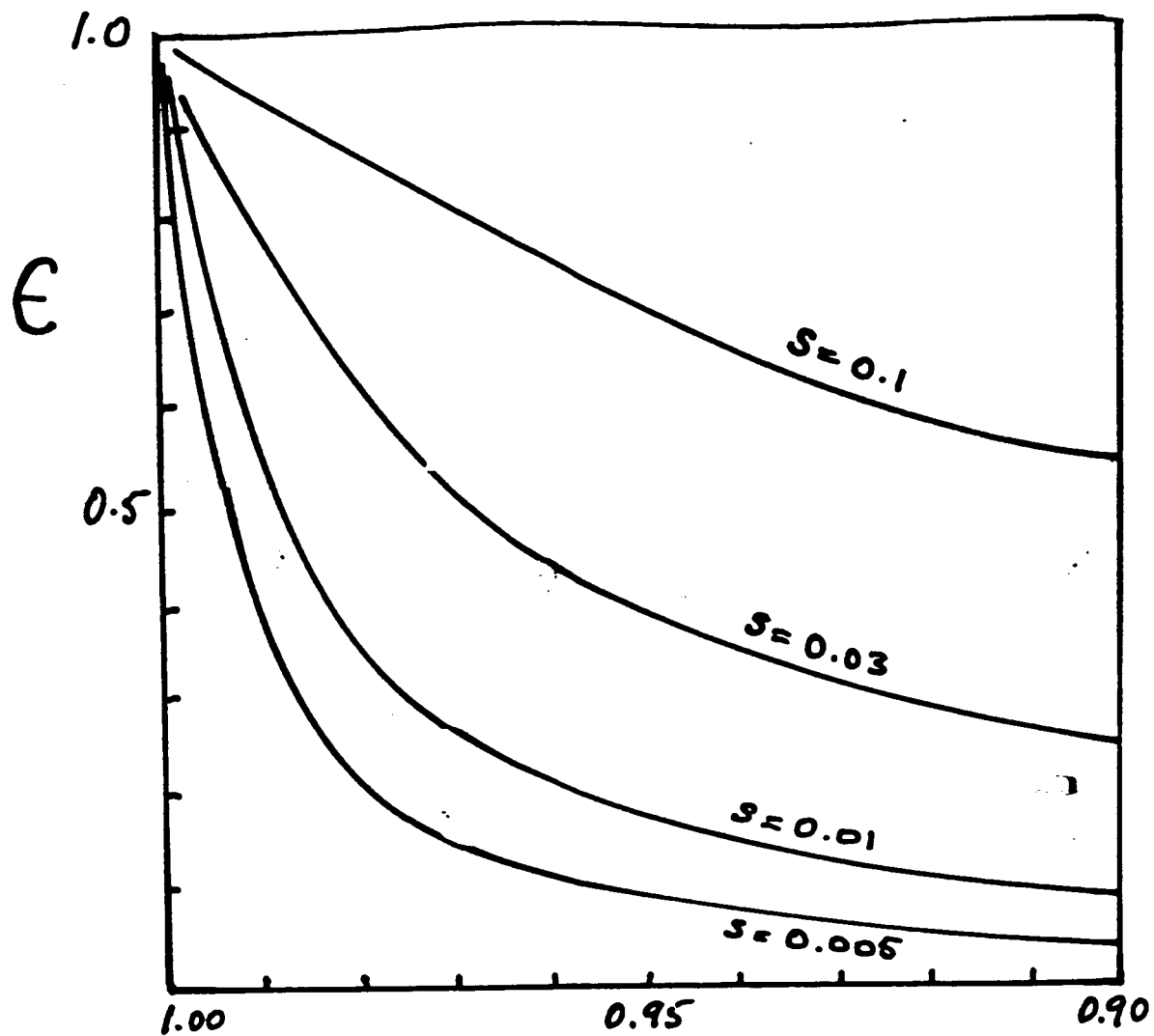


Figure 2. Light-Collection Efficiency, ϵ , vs. Paint Reflectance for Light-Diffusion Boxes. Values given for s-ratios of 0.5% to 10% (s = PMT Face Area/Total Internal Area).

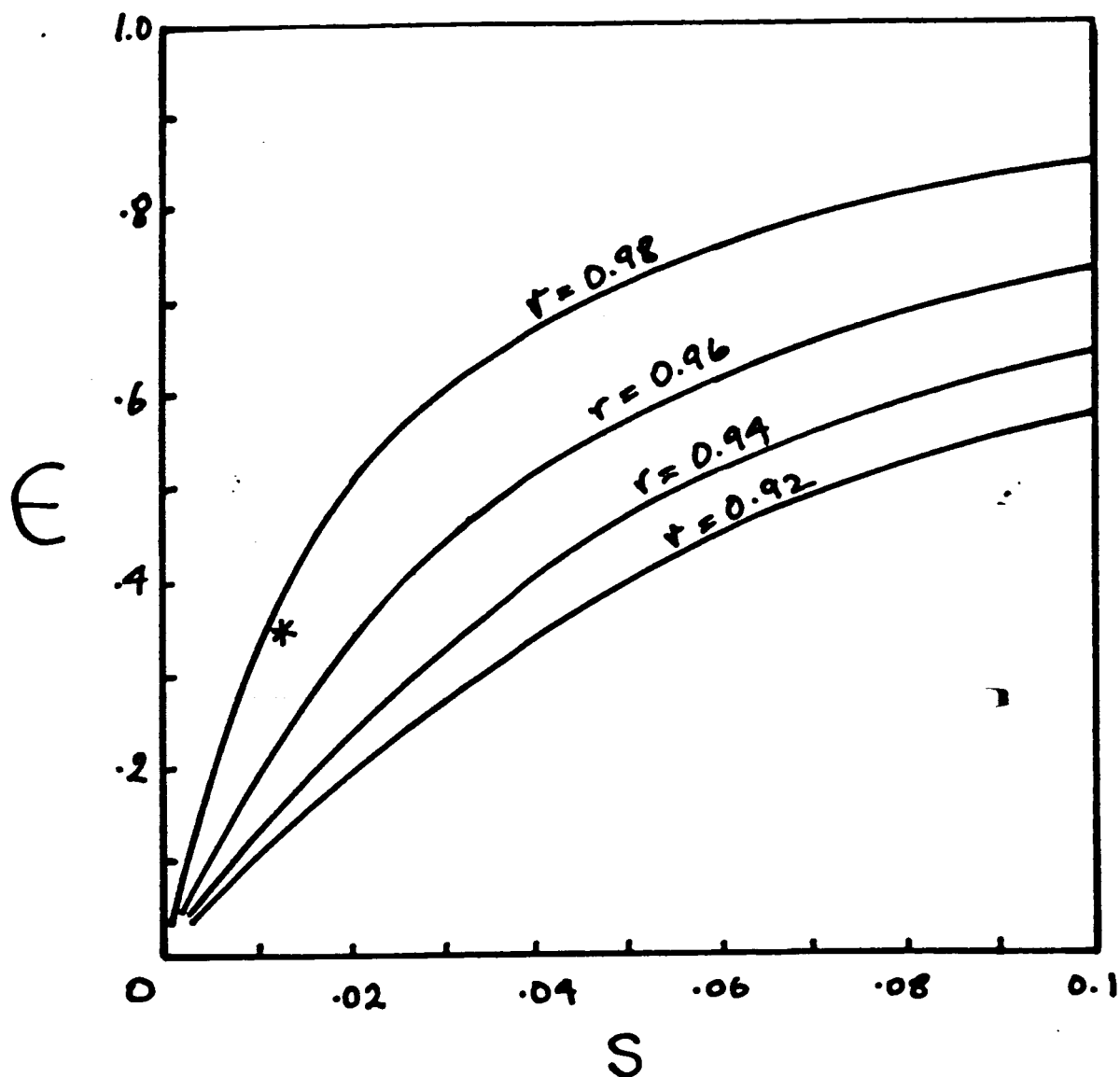


Figure 3. Light-Collection Efficiency, ϵ , vs. s-ratio (s = PMT Area/Total Internal Area). Curves are for Reflectances of 0.92 to 1.0. Asterisk in Data from a Flight Gas-Cerenkov Coated with Good Quality BaSO_4 .

mounted in the side walls. The PMT's with flange hardware were 19 cm in diameter. The nominal dimensions of the box were therefore set at 170 cm x 170 cm x 25 cm.

Design requirements of the box are: sufficient rigidity to support 37 lbs of radiator and 32 lbs of PMT hardware without distortion and rupture, absolute light-tightness, and low weight. The design approach used lightweight foam sandwich technology developed for aerospace use. The core selected was 0.75 inch thick polystyrene foam, clad with 0.006 inch aluminum skins, bonded with a urethane-modified epoxy adhesive (Narmco 7343). The box was fabricated by a modular process, with the 4 sides, the bottom, and the top laid up and bonded separately. The foam core in each element was completely encapsulated, being provided with U-shaped edge members bonded in place on the panel assembly.

Bonding: Adhesive thickness was effectively controlled by transfer rolling in much the same fashion as is employed in inking a printing press, applying adhesive to both surfaces to be mated. Wooden support rings (for detector tube support) were inserted in cut-outs in the foam core, and bonded in the single component assembly process. Other inserts to provide attachment points for the plastic radiators and feed throughs for LED calibrators were placed at this time. Pressure was applied by covering the coated and assembled components with a 3-mil nylon film bag, pumping down, and holding at 20-25 in Hg for 2 days. This process, and subsequent assembly operations, were carried out on a 7' x 7' plywood platen, specially constructed and levelled for the purpose, and sealed to prevent air leaks into the evacuated bag volume.

Assembly: The sides were bonded to the bottom plate with the same adhesive used in sandwich assembly; this bond was reinforced by bonding internal and external angle strips, internally and externally, at each panel juncture. These strips carry the principal load across the joint and add to longitudinal strength to better carry support and landing loads.

The completed box shown in figure 13 had good rigidity and structural strength. Vacuum chamber tests showed that the design was adequate for balloon-flight deployment. PMT and plastic radiator mounting hardware has been fabricated for one unit. Weights of the completed article are

box, unpainted	32 lbs
PMT's, 16 x 2 lbs	32 lbs
plastic radiator	37 lbs
paint, insulation	<u>9 lbs</u>
TOTAL	110 lbs

(Note that the burst detector will need only 4 PMT's.)

The photomultiplier selected for use is the 5" EMI D302B. While this tube is rather temperature sensitive, other attributes of conversion efficiency, ruggedness and low cost recommend it. Temperature sensors will be mounted to the face of the PMT's to monitor temperature variations during flight to allow corrections to the pulse-height data. Fittings for the light-emitting diode (LED) calibrators were fabricated. One will be mounted in the center of the detector for tube balancing and the other in one corner for anisotropy and dynamic range checking. Each LED is mounted in a 2 in. long aluminum tube so that the LED light is directed down into the radiator in a narrow cone and may not be directly viewed by any PMT.

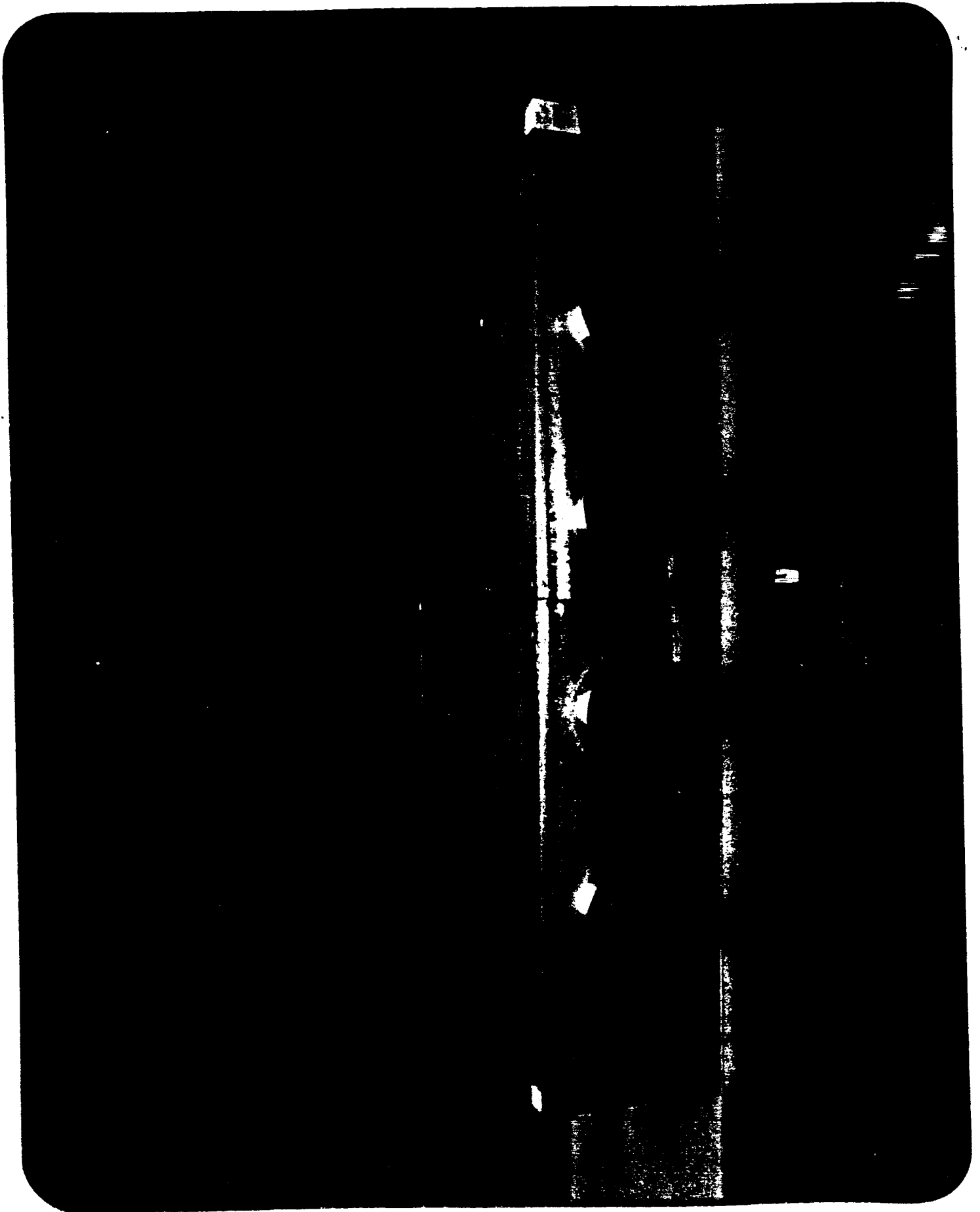


Fig. 4

B. Proportional Counter Hodoscope Design

Proportional counters possess many advantages for use in large area hodoscopes. These include adjustable gain and wide dynamic range of triggering particles, reliability, and relatively low cost. As discussed above, the multiwire counter technology developed at MSFC and successfully used on several balloon flights including JACEE-3 is not suited for application without a heavy enclosing pressure vessel. We have consequently adopted the basic approach of a JACEE group at the Institute for Cosmic Ray Research (ICR), the University of Tokyo, and introduced some improvements to make it suitable for large area hodoscopes. This approach, conceptually shown in figure 5, operates on the same physical principles as that used in JACEE-3 except that the counter gas is now retained by individual thin-walled aluminum tubes in close-packed arrays. An anode wire runs down the center of each tube, from which signals are amplified and processed.

The earliest version of the ICR cellular hodoscope was a 1 m x 1 m model using a soldering method for tube attachment and sealing to the end boxes. Following discussions with ICR personnel two major modifications were adopted. The first was the use of an epoxy construction technique to fuse all tubes together and seal the headers that contain the gas and electronics. The second was the introduction of spring tension on each anode to uniformly tension the anode, so that anode sag under gravity and varying tension due to thermal and structural forces was controlled. A 1.8

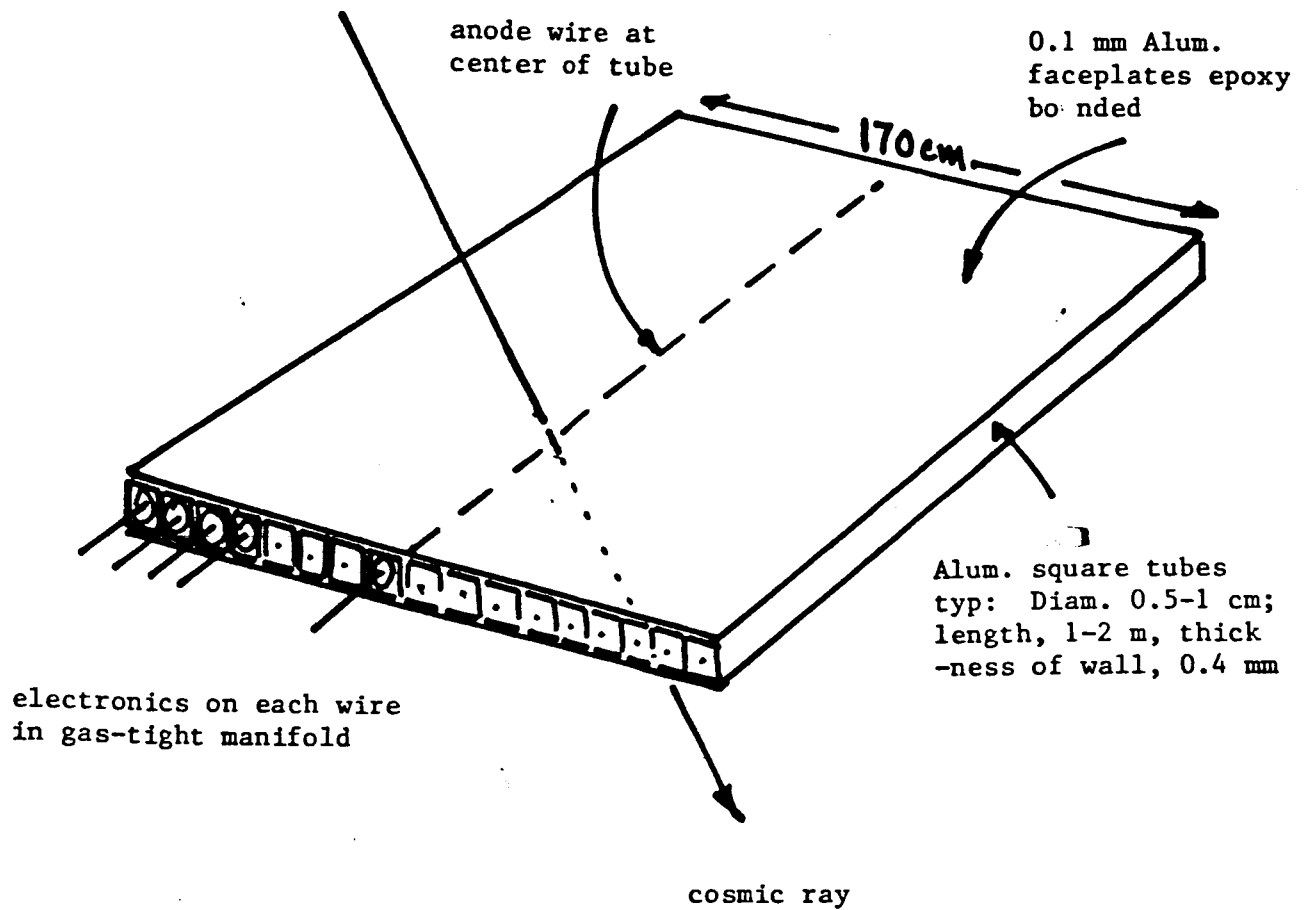


Figure 15. Concepts of Cellular Proportional Counter Hodoscope.

m x 1.8 m version of this hodoscope with these modifications see figure 16 has been fabricated by the CI company of Tokyo, Japan and ICR personnel. It was successfully tested on a balloon flight in Japan in June 1985. Some performance curves from test counters are shown in figures 7, 8, and 9.

The readout of the hodoscope is performed by using high sensitivity discriminators on each anode wire which transfer any received anode signal during a one microsecond gating time to an attached shift register. The shift register has the same number of bits as the number of anodes in the plane, (180 in this case). Following the triggered event the register is shifted through 180 cycles by an external clock and the data is delivered at the clock count corresponding to the anode number. The discriminators and shift register are contained in the headers of each hodoscope layer as shown in figure 6. This allows a minimum number of electrical feed throughs into the gas volume, which is self contained in each plane. Feed throughs are required only for high voltage (~1800 volt), low voltage, clock in, and readout.

Of major importance in the design is the position and angular resolution of the hodoscope. Poorer resolution results in a larger area which must be searched in the CR39 plates and a larger number of background tracks which may be confused with the track of interest. An analysis of this problem is given below in terms of cell size and other instrument parameters.

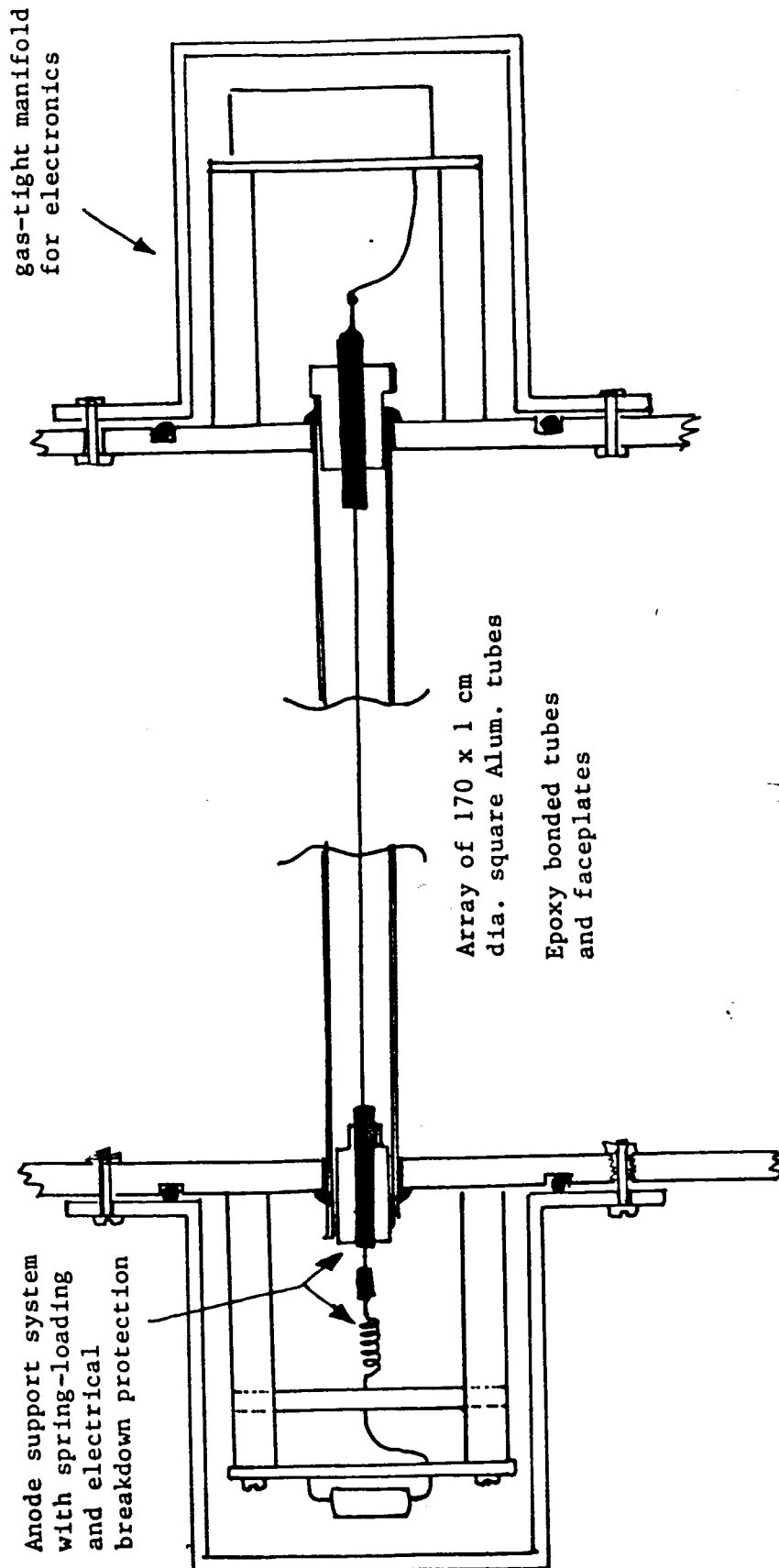


Figure 6. Design Sketch of Cellular PCH

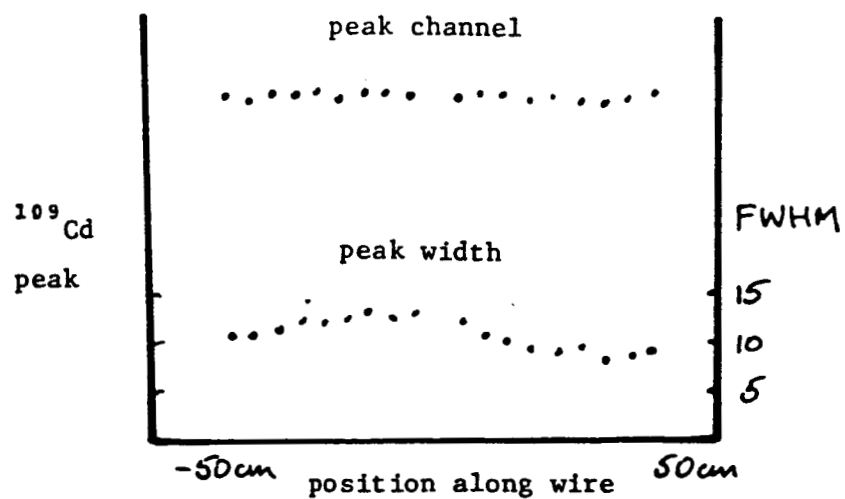


Figure 17. PCH Test Counter Performance (ICR)
Showing Small Gain and Resolution Variation
Along 1 Wire

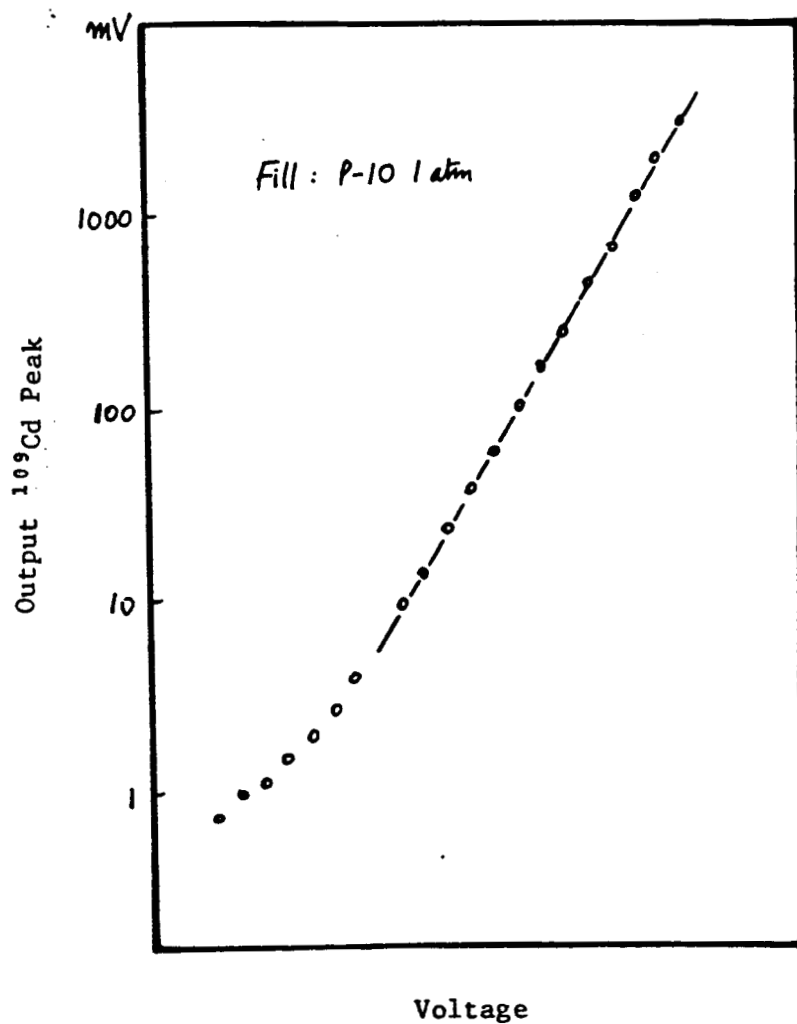


Figure 8. Proportional Behavior of PCH
Test Counter

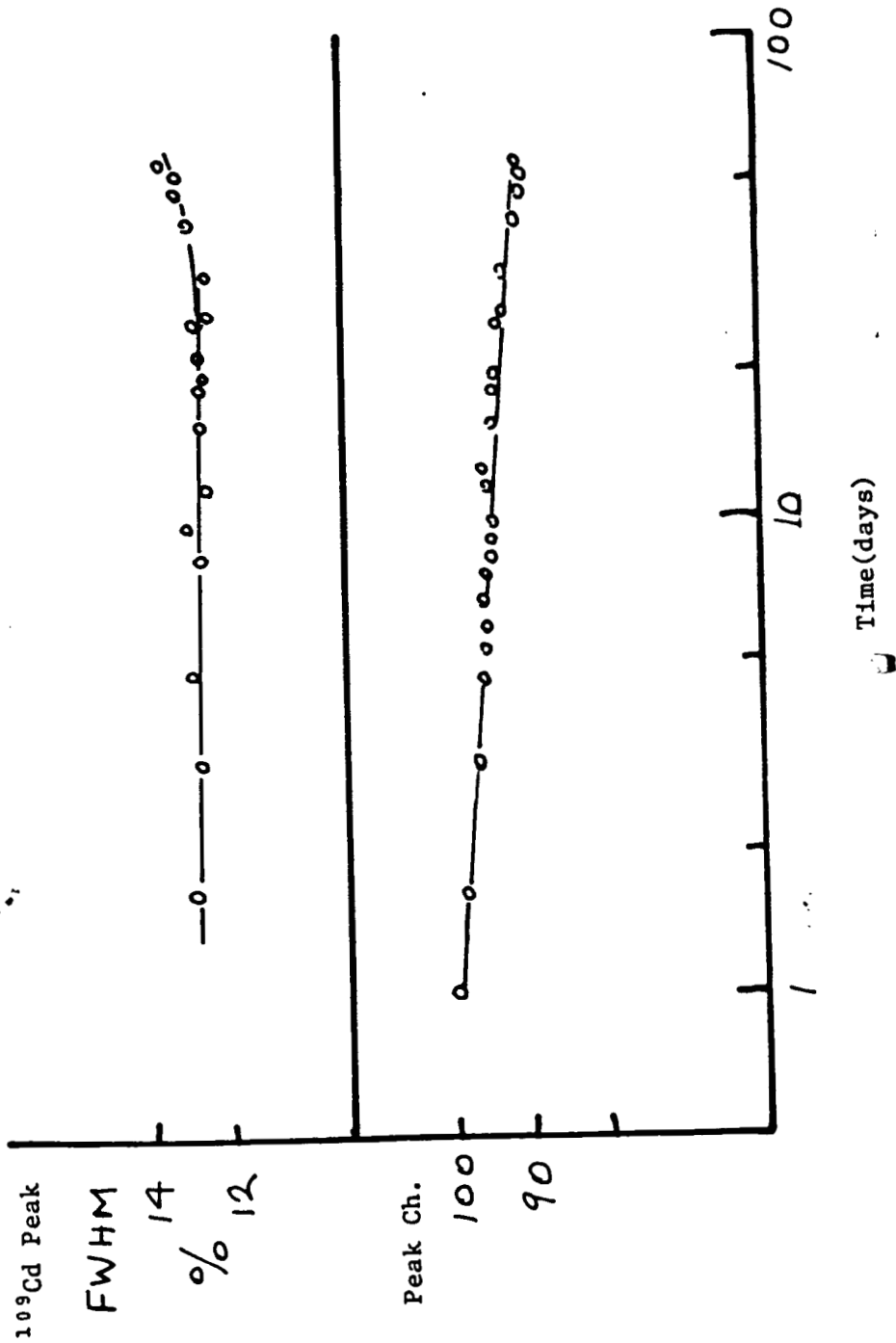
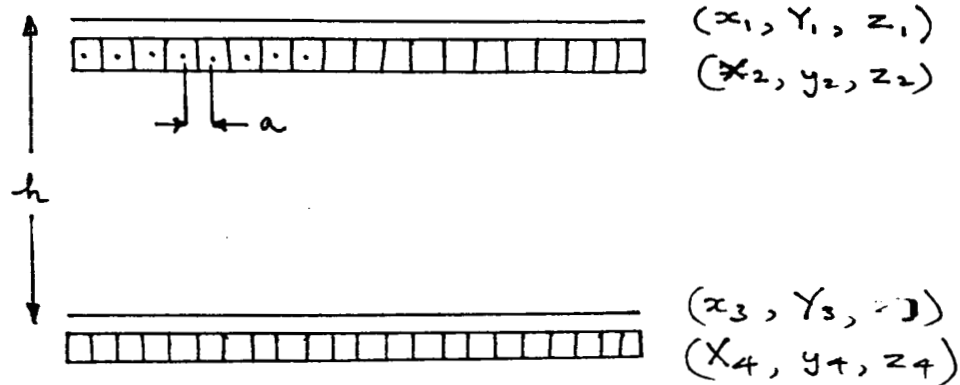


Figure 19. Performance Variation with Time
of PCH Test Counters

(ii) Tracking Error Analysis

The parameters affecting confusion in locating particles chosen by electronic criteria depend on the size of the error region in Δx , Δy , $\Delta \theta$, $\Delta \phi$, Δz and the number of background tracks of similar character within this error box. The background number, for the cosmic rays, depends chiefly on the flight exposure time and the geomagnetic latitude of the flight. Hodoscope parameters may be expressed as shown:



For a given track, zenith angle θ , and azimuthal angle ϕ , y_1 and x_4 are calculated by:

$$\tan \theta = \frac{\sqrt{(x_1 - x_3)^2 + (y_2 - y_4)^2}}{z_3 - z_1} = \frac{\sqrt{(x_1 - x_3)^2 + (y_2 - y_4)^2}}{h}$$

$$\tan \phi = \frac{y_2 - y_4}{x_1 - x_3}$$

$$y_1 = y_2 + (z_1 - z_2) \tan \theta \sin \phi - y + a \tan \theta \sin \phi$$

$$x_4 = x_3 + (z_3 - z_4) \tan \theta \cos \phi = x_3 + a \tan \theta \cos \phi$$

Practically the uncertainty in x , $y \sim a$ (the cell size).

$$\begin{aligned}\text{Then } \sigma(X,Y) &= a \sqrt{1 + 2 \left(\frac{z_1 - z_2}{z_3 - z_1} \right)^2} \\ &= a \sqrt{1 + 2(a/h)^2}\end{aligned}$$

$$\begin{aligned}\sigma(X,Y) &\sim a \text{ for } a \ll h \\ (a &= 1 \text{ cm, } h = 30 \text{ cm in this case})\end{aligned}$$

$$\sigma(\tan \theta) = \frac{\sqrt{2} \cdot a}{h} \quad (\text{constant})$$

$$\sigma(\phi) = \frac{\sqrt{2} \cdot a}{h \tan \theta} \quad \text{radian}$$

The search region is then defined by:

$$\text{Area} = 2a \times 2a = 4a^2$$

$$\text{Solid Angle} = 4 \delta\phi \frac{m \delta m}{(1 + m^2)^2} \quad (\text{where } m \equiv \tan \theta)$$

$$= \frac{8 a^2}{h^2 (1 + m^2)^2} = 8.9 \times 10^{-3} \times \frac{1}{(1 + m^2)^2}$$

$$\Delta\Omega (\text{max}) = 8.9 \times 10^{-3} \text{ steradian (for } m = 0)$$

The requirement for no confusion is that there shall be a density less than 1 particle/ $\Delta A \cdot \Delta\Omega$ to avoid mis-tracking.

Maximum acceptable background of similar tracks

$$= \frac{\pi}{8.9 \times 10^{-3} \times 4} \text{ cm}^{-2}$$

$$= \underline{88 \text{ tracks cm}^{-2}}$$

for the geometry considered here.

Calculated background levels are shown in Table II for two geomagnetic cutoff conditions corresponding to Palestine, Texas, ($R_c = 4.3$ GV) and Hawaii, ($R_c = 13.3$ GV).

Table II

CALCULATED BACKGROUND TRACK DENSITY (30 HOUR FLIGHT)

	$R_c = 4.3$ GV (Tracks/cm ²)	$R_c = 13.3$ GV (Tracks/cm ²)
$Z \geq 17$	13	2.7
Ne-S	36	6.8
C-0	130	27

It is concluded from this analysis that tracks could be correlated between the PCH and the emulsion chamber for elements Ne-Fe without ambiguity for a typical flight from Palestine, Texas. If the flight were at the out-off rigidity of Hawaii, track location would be much easier at all z 's and would be feasible down to CNO.

While it is clear that smaller tube sizes give better resolution and easier tracking, there are practical difficulties to be considered, some of which are:

- increased complexity and weight of electronics which scales with anode wire number.

- difficulties with anode wire sag and array-plane distortion are worse with smaller tube sizes.

A practical limitation for tube-size is in the 5 to 10 mm diameter range for arrays up to 2 m long. This is determined not so much by anode wire sag which is < 1 mm in the center at the proper tension, but by bending of the array under various forces deriving from accumulated anode tension, attachment stresses, differential thermal expansion, and gravity. A tube diameter of 1 cm has been chosen for the design of the flight system.

C. Flight Gondola and Structural Support System

Structural Design Specification

The gondola had to meet the following specifications:

- o ability to support 5000 pounds of payload under balloon launch and parachute opening conditions
- o means for cable attachment
- o cradle system should be included to support gondola and payload before launch
- o minimum weight and cost

Design Description

The instrumentation is supported on a platform suspended from the balloon by cables at the corners. The platform consists of an aluminum honeycomb sandwiched between two aluminum skins. The honeycomb arrangement was chosen for its high structural rigidity and low weight. The skins

distribute the loads more evenly and provide a flat surface for attachment of the emulsion chambers.

The honeycomb is bounded by four C-channels mitered at the corners and adhered to the honeycomb. Cables run from the corners of the C-channels to the balloon. The cables pass through holes in the channels and are swaged to prevent them from pulling through.

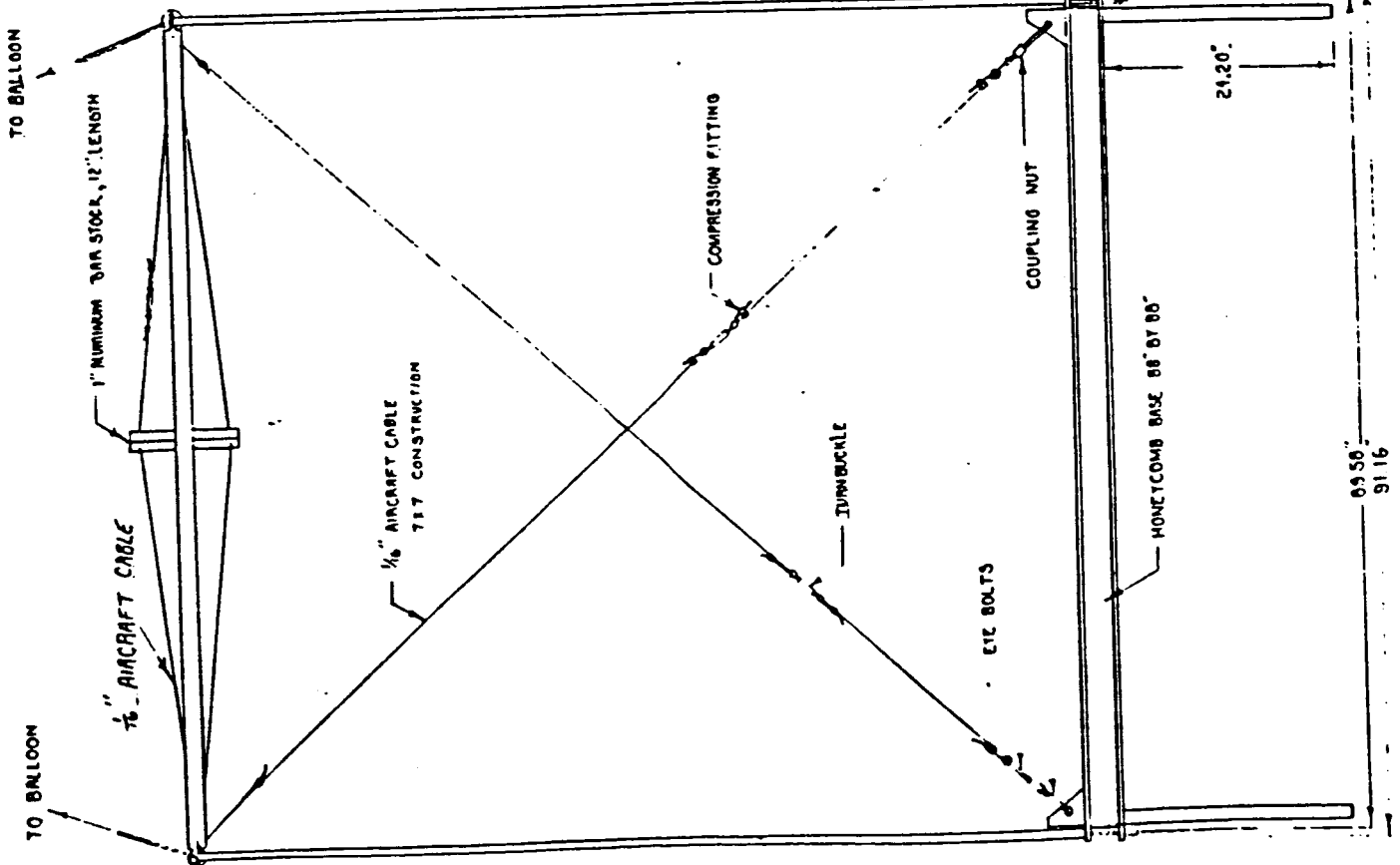
Performance

Complete stress analyses were performed for the components of the structure. Calculations for the more critical elements may be found in the design notebooks. The calculations were performed using conservative, but reasonable factors of safety. A static factor of safety of two was used throughout. An additional dynamic factor of safety of three was imposed on load-bearing members during flight to accomodate parachute-opening shock loads.

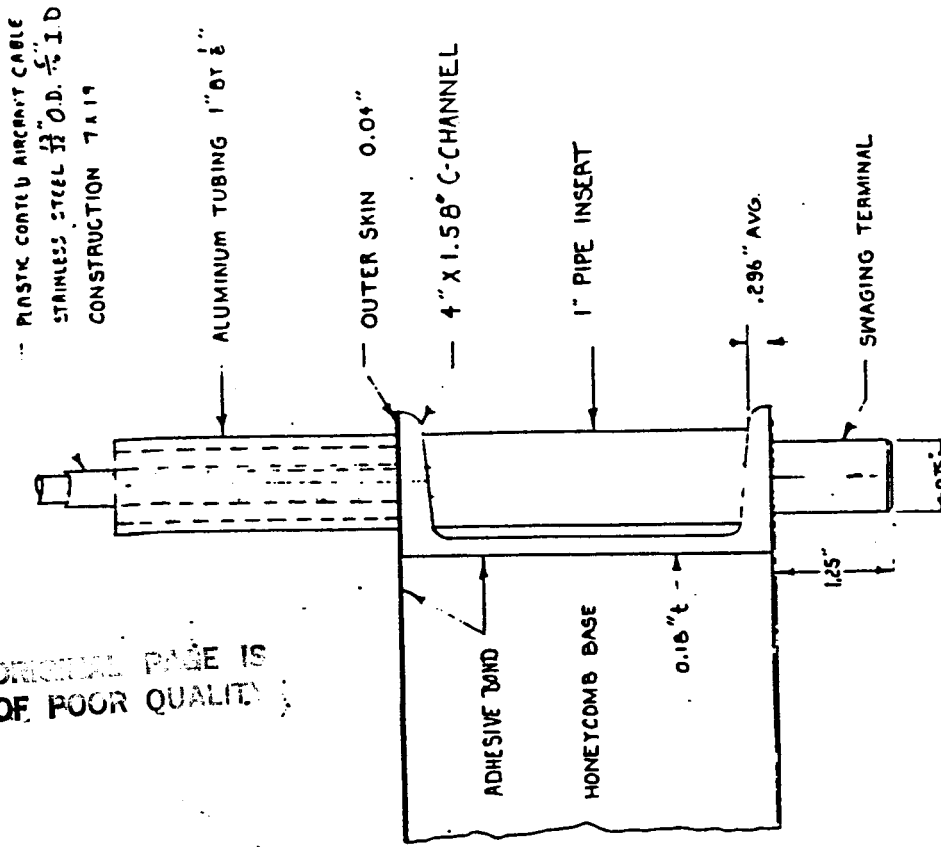
Conclusions

A drawing of the gondola and support system design is shown in figure 10. As this structure is balloon flight hardware a stress and safety analysis is required. The approach used in this design maximizes the possibility of a successful flight.

The design provides rigid supports under the spreader allowing facile ground operations with the cables and spreader attached. If the latter could be left detached until just before launch, the rigid supports could be omitted. The total weight of the support system including cables is 220 lbs.



ORIGINAL PAGE IS
OF POOR QUALITY



DETAIL A-A
10" x 10"

DETAIL A-A

Figure 10. Support-System Design for
Hybrid Instrument

E. INSTRUMENT SUMMARY

EMULSION CHAMBERS9 Chambers, 40 x 50 x 25 cm³

Weight, including boxes

1062 kg

CHARGE COUNTERDiffusion Box 170 x 170 x 25 cm³

16 D302B PMT's, Analyzed in 4 Banks

Radiator 150 x 150 x .635 cm Pilot 425

Weight

50 kg

Burst CounterDiffusion Box 170 x 170 x 25cm³

4 D302B PMT's, Individually analyzed

Radiator 150 x 150 x .635 cm Plastic

Scintillator

Weight

41 kg

Hodoscopes

Cellular PCH, 3 x Y pairs

1 cm square tubes filled with P10 gas
resolution 1 cm² and 2°

Weight

150 kg

Support Structure

Honeycomb Platform, Struts

Weight

115 kg

Electronics, Batteries(Preamps, amps, discriminators, ADC's
Triggering System, Calibration,
Housekeeping, Digital Data, High
Voltage)

Weight

78 kg

TOTAL WEIGHT, SCIENTIFIC INSTRUMENT

1486 kg
(3270 lbs)